Available online at www.sciencedirect.com

ScienceDirect

Mendeleev Commun., 2021, **31**, 561–563

Mendeleev Communications

Role of oxides in the electrochemical dissolution of Pd and its alloys

Boris I. Podlovchenko,* Yurii M. Maksimov, Tatyana D. Gladysheva and Dmitry S. Volkov

Department of Chemistry, M. V. Lomonosov Moscow State University, 119991 Moscow, Russian Federation. Fax: +7 495 939 0171; e-mail: podlov@elch.chem.msu.ru

DOI: 10.1016/j.mencom.2021.07.042

The dissolution of Pd, Pd–Pb and Pd–Cu electrodeposits proceeds predominantly from the surface free from chemisorbed oxygen. The strongest inhibiting effect of surface oxides is revealed in the dissolution of the mixed deposits.

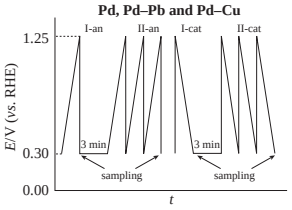

Keywords: electrodeposit, Pd, Pd–Pb, Pd–Cu, electrodissolution, anodic potential, surface oxide.

Employment of Pd catalysts in fuel cells is hampered by their cost as well as lower corrosion stability compared with other noble metals.[1–6] The Pd corrosion is typically explored using cyclic voltammetry, with some reports considering the predominant anodic dissolution of Pd in the corresponding potential scan[2,7–9] and other works demonstrating the preferential transfer to solution in the course of cathodic desorption of oxides.[10–13] The opinions on how a non-noble metal additive affects the Pd corrosion stability are still controversial,[1,5,6,14–17] the dispersed forms of Pd catalysts being the least explored.[1–4,18]

We investigated the dissolution of dispersed electrodeposited Pd and Pd–M (M = Pb, Cu) in anodic potential scan, the process was found to be limited by the formation of monolayer of palladium oxide,[5,19] though the role of oxides in the dissolution was not considered. Therefore, it is of interest to compare these results with the ones using the same samples and analogous conditions but in a cathodic potential scan.

In this work, the electrodeposits of Pd–Pb and a Pd reference were obtained from deaerated solutions of $Pb(ClO_4)_2$ + $PdCl_2$ + + 0.1 M $HClO_4$ and $PdCl_2$ + 0.1 M $HClO_4$, respectively, at the deposition potential E_{dep} of 100 mV,[5] while Pd–Cu and the corresponding Pd reference were electrodeposited from solutions of $CuSO_4$ + $PdSO_4$ + 0.5 M H_2SO_4 and $PdSO_4$ + 0.5 M H_2SO_4, respectively, at E_{dep} = 400 mV, all potentials from here on being given relative to reversible hydrogen electrode (RHE) in the same solution. For one group of samples, the electrodissolution was carried out in a slow anodic potential scan from 0.3 to 1.25 V followed by a quick drop back to 0.3 V,[3] for another group a slow cathodic potential scan from 1.25 to 0.3 V was preceded by a potential jump from 0.3 to 1.25 V. The linear potential scan rate was 1.7–2.0 mV s^{-1}. The resulting four dissolution modes are demonstrated in Figure 1, the I-an and I-cat modes being called anodic and cathodic half-cycles, respectively. Use of the anodic half-cycles allowed one to eliminate the dissolution and redeposition of Pd in the cathodic scan, which occurred when the full-cycle voltammogram (CVA) was recorded, whereas the employment of the cathodic half-cycles made it possible to avoid the dissolution in the anodic scan (for details, see Online Supplementary Materials, S1). The amount of Pd passed to solution after the polarization of electrodeposited Pd was estimated using ICP-AES (Table 1).

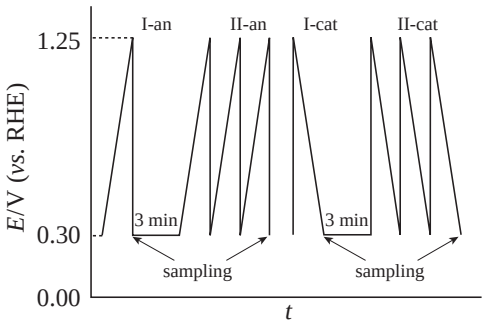

Figure 1 Four dissolution modes employed and their corresponding potential variations in electrochemical dissolution of electrodeposited Pd and Pd–M (M = Pb, Cu).

At first sight, it is quite unexpected that the amount of Pd dissolved in three half-cycles in mode II differs little from the corresponding amount in one half-cycle in mode I. However, it should be taken into account that the first half-cycle pertains to a freshly formed surface. As follows from Table 1, the dissolution of Pd in a cathodic half-cycle is *ca.* 2–4 times weaker compared with its anodic counterpart.

The dissolution of Pd in the potential range of Figure 1, which is limited on the top by formation of the monolayer of PdO at 1.25 V,[4,20] proceeds through the following reactions:

$$Pd \rightarrow Pd^{2+} - 2\bar{e}\ E_0 = 0.987\ V \quad (1)$$

$$PdO + 2H^+ \rightarrow Pd^{2+} + H_2O, \quad (2)$$

Table 1 Dissolution of Pd (E_{dep} = 100 mV) in 0.1 M $HClO_4$ and Pd (E_{dep} = = 400 mV) in 0.5 M H_2SO_4.

Sample	Mode	Pd dissolved/μg
Pd electrodeposited at 100 mV	I-an	14.2
	II-an	15.0
	I-cat	7.8
	II-cat	5.2
Pd electrodeposited at 400 mV	I-an	2.1
	I-cat	0.54

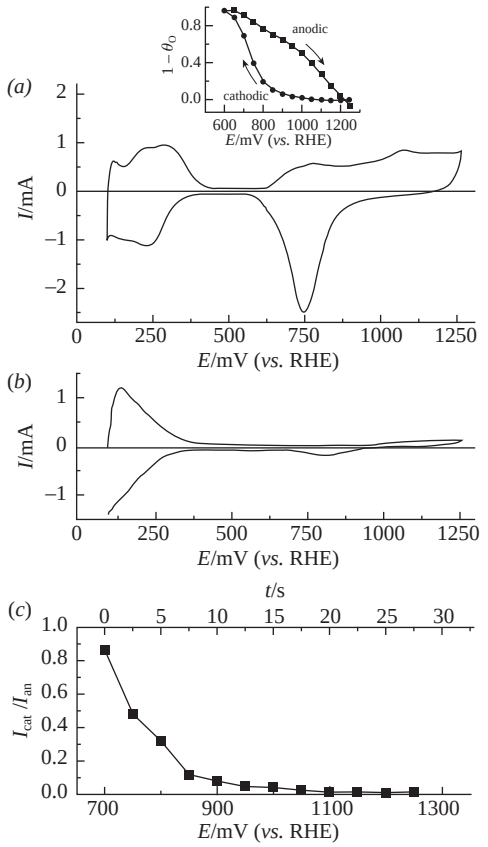

Figure 2 (*a*) CVA curve measured in 0.1 M $HClO_4$ at 20 mV s^{-1} for Pd electrodeposited at 100 mV; inset: surface fraction free of chemisorbed oxygen ($1 - \theta_O$) *vs.* potential as determined from the CVA curve in $HClO_4$. (*b*) CVA curve in 0.5 M H_2SO_4 at 7 mV s^{-1} for Pd electrodeposited at 400 mV. (*c*) Hypothetical ratio $I_{cathodic}/I_{anodic}$ of Pd dissolution currents in the anodic and cathodic half-cycles *vs.* potential.

while the formation of PdO, as a result of the reaction $Pd + H_2O \rightarrow$ $\rightarrow PdO + 2H^+ + 2\bar{e}$, proceeds with the rate far exceeding the dissolution velocity of Pd.[2–4]

Figure 2 demonstrates typical CVA results for the Pd deposits. As is known,[1–4] the dissolution of Pd starts at *ca.* 700 mV. The monolayer of chemisorbed oxygen (PdO) begins to form in the anodic potential scan also at 700–800 mV. Thus, in the anodic half-cycles, dissolution of Pd proceeds under the conditions when a considerable surface fraction is free from palladium oxide. For more than a half of the cathodic half-cycle at *ca.* 1250–950 mV, the dissolution proceeds on the surface almost completely occupied by PdO. Even when the potential value of 700 mV is attained, the oxide still remains on a considerable part of the surface. Therefore, a higher total dissolution rate in the cathodic scan is expected if Pd dissolves preferentially by the reaction (2).

The ratio of Pd dissolution currents in the cathodic ($I_{cathodic}$) and anodic (I_{anodic}) scans can be roughly assessed by assuming that it occurs only in the areas unoccupied by PdO. Let us suppose that irrespective of the scan direction, the Pd dissolution current is a certain function of potential $I = f(E)$ $(1 - \theta_O)$, where $(1 - \theta_O)$ represents the surface fraction free of chemisorbed oxygen. Then, $I_{cathodic}/I_{anodic} = (1 - \theta_O)_{cathodic}/(1 - \theta_O)_{anodic}$. The ratio of the Pd surface fractions unoccupied by oxygen in the anodic and cathodic scans was tentatively estimated from the curve in Figure 2(*a*), where contribution of the Pd dissolution currents was neglected due to high potential scan rate.[3,4] We assumed the $(1 - \theta_O)$ values as 1 and 0 at 0.6 and 1.25 V, respectively. The quantities of electricity consumed in the potential scanning up to the required values were normalized to the charge obtained by integrating the cathodic peak for the reduction of chemisorbed oxygen. The inset in Figure 2(*a*) demonstrates the $(1 - \theta_O)$ values found in the anodic and cathodic scans. The ratios $I_{cathodic}/I_{anodic}$ calculated based on these values for potentials range of 0.7–1.25 V, where the Pd dissolution is possible, are presented in Figure 2(*c*), with the time scale for potential scanning from E = 700 mV being shown on the top. In the range of 950–1250 mV where we expect the greatest values for the $f(E)$ function according to reaction (1), the ratio $I_{cathodic}/I_{anodic}$ is close to zero. The currents become commensurable only in the range of 0.7–0.85 V, where they themselves are low. These calculations confirm the assumption that in the potential range under investigation, the Pd dissolution proceeds predominantly by reaction (1). Were Pd dissolution by reaction (2) impossible, one could expect even greater differences between the dissolution in the anodic and cathodic half-cycles compared with the ones observed (see Table 1). Note that these calculations cannot be employed for the quantitative analysis of experimental data on the dissolution because they have been obtained at the potential scan rate one order of magnitude lower than the rate used in recording the CVA curve in Figure 2(*a*). Moreover, the factors like possible formation of an incomplete PdO monolayer at 1.25 V[4] as well as probable activation of the catalyst surface upon desorption of chemisorbed oxygen[21] were ignored, while both of them could accelerate the Pd dissolution in the cathodic potential scan.

Figure 3 demonstrates typical CVA curves for freshly electrodeposited Pd–Pb and Pd–Cu. In the potential range of interest exceeding 700 mV, these curves differ from their counterparts for electrodeposited Pd (see Figure 2). First of all, this is manifested in higher current observed for the mixed deposits, which is associated with an increase in the degree of dispersion of Pd deposits with introduction of Pb and Cu.[5,19] The form of the anodic scan is different, which is associated with a change in the energy spectrum of oxygen chemisorbed on Pd, formation of mixed oxides $PdMO_x$[22] and definite dissolution of metals. Certainly, the effect of increase in current during the anodic potential scan in the presence of Pb or Cu is associated in some extent with anodic leaching of the non-noble metals from their alloys. The total contribution of such currents makes it possible to assess the observed dissolution of Pb and Cu from the mixed deposits. The calculation results in less than 15% of the total charge in the oxygen region of curves in Figure 3 (for details, see Online Supplementary Materials, S2).

Table 2 illustrates the dissolution of electrodeposited Pd–Pb and Pd–Cu in anodic and cathodic half-cycles (see Figure 1) according to ICP-AES data. The effect of weaker dissolution of Pd in cathodic half-cycles compared with anodic ones (5–7 fold for electrodeposited Pd–Pb and *ca.* 20 fold for Pd–Cu) is more pronounced for the mixed deposits.

Thus, the preferential dissolution of Pd in the surface areas free of chemisorbed oxygen (oxides) is higher when the second component is present in the deposit, probably due to formation of mixed

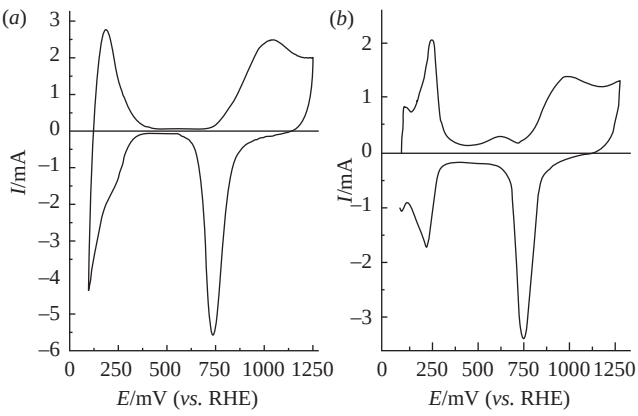

Figure 3 CVA curves (*a*) in 0.1 M $HClO_4$ at 20 mV s^{-1} for electrodeposited Pd–Pb and (*b*) in 0.5 M H_2SO_4 at 7 mV s^{-1} for electrodeposited Pd–Cu.

Table 2 Dissolution of electrodeposited Pd–Pb in 0.1 M $HClO_4$ and electrodeposited Pd–Cu in 0.5 M H_2SO_4 in half-cycles as well as under potentiostatic conditions.

Sample	Mode	Pd dissolved/μg	Pb or Cu dissolved/μg
Pd–Pb electrodeposited at 100 mV	I-an	36.6	49.2
	II-an	41.7	29.1
	I-cat	7.0	4.2
	II-cat	5.8	3.5
	1.1 V, 5 h (potentiostatic)	4.5	3.2
Pd–Cu electrodeposited at 400 mV	I-an	7.1	3.1
	I-cat	0.34	0.64
	1.1 V, 6 h (potentiostatic)	0.58	1.0

oxides $PdPbO_x$ or $PdCuO_y$. The potential of cathodic peak in the CVA curves of electrodeposited Pd–Pb is 690 ± 15 mV compared with 740 ± 10 mV for reference Pd deposited at 100 mV, while for Pd–Cu it is 710 ± 15 mV in contrast to 780 ± 10 mV for Pd deposited at 400 mV. This allows one to suggest that the bond between oxygen and the surface becomes stronger upon incorporation of Pb or Cu into Pd.

Note that the long term polarization for 5–6 h of electrodeposited Pd–Pb and Pd–Cu under potentiostatic conditions at 1.1 V produced the one order of magnitude smaller amount of Pd passed to solution compared with the one in the anodic half-cycles (see Table 2), although the time the deposits spent in the potential range of 0.7–1.25 V for even three half-cycles was not more than *ca*. 0.25 h. At 1.1 V the surface of electrodeposited Pd and Pd–M was occupied by oxides to the large extent. In the cathodic half-cycles of the mixed Pd deposits, the second components also dissolved weaker (see Table 2, right column), which additionally confirms the inhibiting effect of oxides on the dissolution of the deposits.

The above results reveal that in the potential range of formation of a monolayer of chemisorbed oxygen (PdO), it considerably inhibits the Pd dissolution, which agrees in general with the mechanism of Pd dissolution deduced from electrochemical scanning flow cell measurements combined with on-line ICP-MS,[3] though, in contrast to the authors of study,[3] we assume here that the partial dissolution of Pd proceeds as well through the reaction of PdO with its acidic environment according to reaction (2).

In summary, the inhibiting effect of oxides on the Pd dissolution becomes stronger in the presence on the surface of a non-noble metal as the second component. This explains high stability of mixed Pd–M electrocatalysts in the oxygen reduction reaction, which proceeds in acidic solutions at the potentials of practical interest, namely ⩾0.8 V, with considerable surface coverage by oxides.

This work was supported by the Russian Foundation for Basic Research (project no. 19-03-00309) and in part by the M. V. Lomonosov Moscow State University Program of Development (the state assignment no. AAAA-A21-121011590088-4).

Online Supplementary Materials

Supplementary data associated with this article can be found in the online version at doi: 10.1016/j.mencom.2021.07.042.

References

1 H. Meng, D. Zeng and F. Xie, *Catalysts*, 2015, **5**, 1221.
2 D. A. J. Rand and R. Woods, *J. Electroanal. Chem. Interfacial Electrochem.*, 1972, **35**, 209.
3 E. Pizzutilo, S. Geiger, S. J. Freakley, A. Mingers, S. Cherevko, G. J. Hutchings and K. J. J. Mayrhofer, *Electrochim. Acta*, 2017, **229**, 467.
4 Yu. M. Maksimov, A. V. Smolin and B. I. Podlovchenko, *Russ. J. Electrochem.*, 2007, **43**, 1412 (*Elektrokhimiya*, 2007, **43**, 1493).
5 B. I. Podlovchenko, Yu. M. Maksimov, D. S. Volkov and S. A. Evlashin, *J. Electroanal. Chem.*, 2020, **858**, 113787.
6 V. V. Kuznetsov, A. V. Telezhkina and B. I. Podlovchenko, *Mendeleev Commun.*, 2020, **30**, 772.
7 A. E. Bolzán, M. E. Martins and A. J. Arvía, *J. Electroanal. Chem. Interfacial Electrochem.*, 1984, **172**, 221.
8 K. Juodkazis, J. Juodkazytė, B. Šebeka, G. Stalnionis and A. Lukinskas, *Russ. J. Electrochem.*, 2003, **39**, 954 (*Elektrokhimiya*, 2003, **39**, 1067).
9 L. M. Vracar, D. B. Sepa and A. Damjanovic, *J. Electrochem. Soc.*, 1987, **134**, 1695.
10 A. E. Bolzán and A. J. Arvia, *J. Electroanal. Chem.*, 1992, **322**, 247.
11 T. Solomun, *J. Electroanal. Chem. Interfacial Electrochem.*, 1987, **217**, 435.
12 B. R. Shrestha, A. Nishikata and T. Tsuru, *Electrochim. Acta*, 2012, **70**, 42.
13 S. H. Cadle, *J. Electrochem. Soc.*, 1974, **121**, 645.
14 O. Savadogo, K. Lee, K. Oishi, S. Mitsushima, N. Kamiya and K.-I. Ota, *Electrochem. Commun.*, 2004, **6**, 105.
15 M. R. Tarasevich, V. A. Bogdanovskaya, L. N. Kuznetsova, A. D. Modestov, B. N. Efremov, A. E. Chalykh, Yu. G. Chirkov, N. A. Kapustina and M. R. Ehrenburg, *J. Appl. Electrochem.*, 2007, **37**, 1503.
16 B. I. Podlovchenko and Yu. M. Maksimov, *J. Electroanal. Chem.*, 2017, **801**, 319.
17 B. I. Podlovchenko, Yu. M. Maksimov, K. I. Maslakov, D. S. Volkov and S. A. Evlashin, *J. Electroanal. Chem.*, 2017, **788**, 217.
18 B. I. Podlovchenko, Yu. M. Maksimov and D. O. Shkil, *Mendeleev Commun.*, 2019, **29**, 312.
19 B. I. Podlovchenko, T. D. Gladysheva, Y. M. Maksimov, D. S. Volkov and K. I. Maslakov, *J. Solid State Electrochem.*, 2020, **24**, 1439.
20 M. W. Breiter, *J. Electroanal. Chem. Interfacial Electrochem.*, 1977, **81**, 275.
21 R. R. Adžić and A. V. Tripković, *J. Electroanal. Chem. Interfacial Electrochem.*, 1979, **99**, 43.
22 B. I. Podlovchenko, T. D. Gladysheva, Yu. M. Maksimov, K. I. Maslakov and D. S. Volkov, *J. Electroanal. Chem.*, 2019, **840**, 376.

Received: 3rd February 2021; Com. 21/6442